Thresholding techniques for segmentation of atherosclerotic plaque and lumen areas in vascular arteries

T. MARKIEWICZ[1,2,*], M. DZIEKIEWICZ[3], S. OSOWSKI[2,4], M. MARUSZYNSKI[3],
W. KOZLOWSKI[1], and R. BOGUSLAWSKA-WALECKA[5]

[1] Department of Pathology, Military Institute of Medicine, 128 Szaserow St., 04-141 Warsaw, Poland
[2] Department of Electrical Eng. Theory, Information and Measurement Systems, Warsaw University of Technology,
1 Politechniki Sq., 00-661 Warsaw, Poland
[3] Department of Vascular Surgery, Military Institute of Medicine, 128 Szaserow St., 04-141 Warsaw, Poland
[4] Military University of Technology, 2 Kaliskiego St., 00-908 Warsaw, Poland
[5] Department of Radiology, Military Institute of Medicine, 128 Szaserow St., 04-141 Warsaw, Poland

Abstract. The paper develops the automatic methods of segmentation of the blood vessel area in the images of the multi-slice computed tomography, allowing to separate the lumen from the atherosclerotic plaque areas. The solution is based on the application of different implementations of thresholding, including between class variance in a bimodal mode, Gaussian mixture modeling, clustering technique, polynomial and multilayer perceptron approximations. These methods are compared with many examples of arteries of different percentage of the plaque occupancy in the iliac and femoral arteries. The numerical results of segmentation have been verified by the medical experts and prove its usefulness in medical practice. The presented system can find application in an automatic evaluation of the atherosclerosis progression/regression of patients on the basis of sequence of Computed Tomography slice images.

Key words: image processing, thresholding methods, computed tomography, vascular image parameterization.

1. Introduction

Thresholding is an important technique for image segmentation, that tries to identify and extract different objects existing in the image by the analysis of the distribution of gray levels or texture in image objects. In spite of existence of many segmentation methods, such as edge detection, region growing, texture analysis, morphological watershed approaches or multi-spectral techniques [1–6] the thresholding is still regarded as the most efficient segmentation approach in medical applications. The thresholding techniques are generally based on either histogram or local properties of the image, such as mean, standard deviation or gradient. If technique is dependent on, say, a local average gray value, it is called "local". In this method the image is usually split into sub-images followed by the calculation of thresholds for each sub-image, or examining image intensities in the neighborhood of each pixel.

On the other side, when only one threshold is selected for an entire image, the technique is said to be "global" and is applicable to the images of the bimodal histogram. If an image contains more than two types of regions, it may still be possible to segment it by applying several individual thresholds, or by using a multi-thresholding technique. With the increased number of threshold values, the histograms become difficult to distinguish and hence thresholding may be no longer optimal.

For medical imaging purposes segmentation is used to extract specific organs, vascular structures, tissue types (e.g. in brain: grey, white, ventricles/CSF), or lesions. At such a variety of problems no single segmentation technique can produce satisfactory results. The difficulties in thresholding approaches to segmentation of medical images follow from the low contrast between different objects, noise or significant changes of the same objects within different images. All of these factors appear usually at the same time in medical images.

This paper considers and compares the application of different techniques to the automatic recognition of the atherosclerotic plaque areas from the lumen in the vascular arteries in the sequence of the multi-slice computed tomography (MSCT) images. Such task belongs to very difficult problems [7–9], since the difference of intensities in both regions is of fuzzy character and at the same time great changes between them are observed in the analyzed sequence of images.

Most thresholding techniques are based on the statistics of the one-dimensional histogram of gray levels [10–12]. For instance, Otsu's between-class variance (BCV) method chooses the optimal thresholds by maximizing the variance between classes with an exhaustive search [11, 13]. Many variations of Otsu method have been proposed in the past. The review of them may be found in the book [14]. The other methods include the clustering approaches [14, 15], minimum error thresholding [10] and Gaussian Mixture Modeling (GMM) [14]. All of them are based on the histogram and frequency of appearing the particular intensity levels in the image. In this paper we compare these traditional approaches to the proposed method based on the polynomial and multilayer perceptron approximations of the sorted pixel intensities.

*e-mail: markiewt@iem.pw.edu.pl

We present the comparison of them on the examples of segmentation of the iliac and femoral artery areas appearing in the images of the MSCT sequence. These arteries are identified automatically in the image slice by using the program developed by us, which is based on the extended regional maxima [4]. In this paper we assume that the artery area has been already identified.

2. Methods

The recognition between lumen and plaques in the vascular arteries represents a difficult problem, since the plaque region is usually non-uniform, differing greatly in intensity, and often resembles lumen. This is especially true in the case of the non-calcified plaques, slightly differing from the lumen. The most important problem in our task is determination of the optimal threshold value, on the basis of which the division of the artery area into lumen and plaque regions is done.

In this work we have implemented and compared different approaches to the determination of an optimal threshold value, allowing for the best separation between lumen and plaque areas. The first approach, proposed by us, uses the approximation of the sorted pixel intensities, implemented here by using polynomial and multilayer perceptron (MLP) approximating functions. The other methods taken into account in this work include: application of BCV, K-means clustering and GMM based thresholding. Careful analysis of these techniques allows to select these, which are the most appropriate for the task of vascular artery area segmentation. Their common use in the analysis of the atherosclerosis of the blood vessels leads to the increase of the accuracy of segmentation and in consequence allows the numerical parameterization of the analyzed images.

2.1. The polynomial fitting of the sorted pixel intensities. The starting point in this procedure is the sorted sequence of pixel intensities. The switching from lumen to plaque is seen in this sorted sequence as a visible bending point of differing slope (see Fig. 1). Analyzing many images we have found that the sorted pixel intensities for the extracted artery plane have a very characteristic distribution. The region of pixels corresponding to plaques had higher slope and larger variance than that corresponding to pixels forming the lumen area.

The easiest way to find the point of the abruptly changing slope of the sorted pixel intensity sequence is through the calculation of the derivative of such a sequence. The derivative curve depicts the significant change of the slope at the border of lumen and plaque areas, easy in automatic recognition. Although direct numerical calculation of the derivative by using the local computation is theoretically possible, we have applied the functional fitting of the sorted pixel intensity curve, avoiding in this way the problem of non-continuity of the results following from the noise. We have used the polynomial curve fitting function described in the form

$$f(x) = a_n x^n + a_{n-1} x^{n-1} + ... + a_1 x + a_0 \qquad (1)$$

fitted by the least-squares method. Its derivative is explicitly given by the relation

$$\frac{df(x)}{dx} = na_n x^{n-1} + (n-1)a_{n-1} x^{n-2} + ... + a_1. \qquad (2)$$
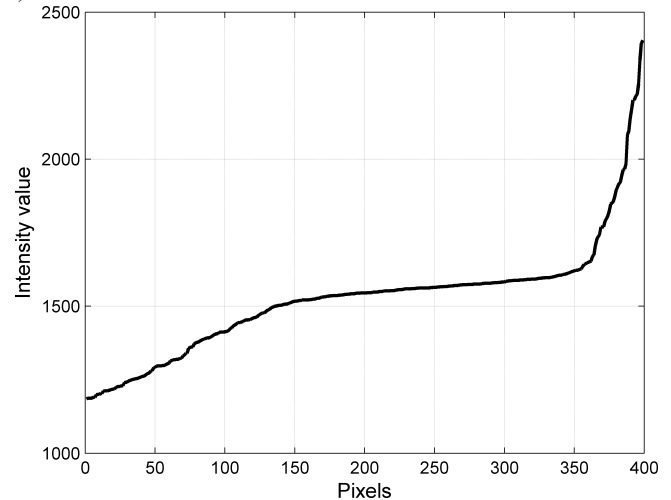
a)
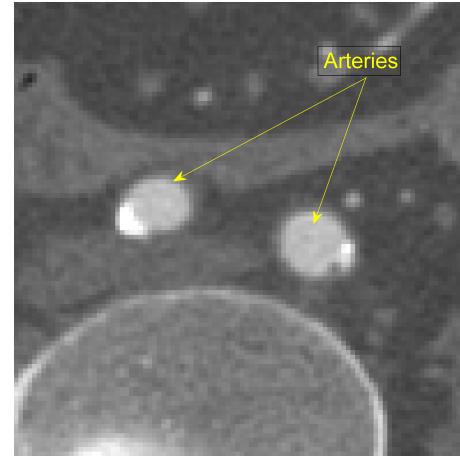
b)

Fig. 1. The representation of the vascular artery area (left and right arteries) by the sorted pixel intensity distribution: a) the real image of the cross section of the two artery areas containing plaques, b) the sorted pixel intensity distribution of these two arteries

The region of the fast increase of the value of the first derivative of this polynomial shows the optimal threshold discriminating the artery lumen from the calcified plaques. On the basis of many experiments concerning different shapes and compositions of lumen and plaque areas, performed for 50 selected MSCT images we have come to conclusion that the appropriate threshold value leading to the proper segmentation of the calcified atherosclerotic plaque areas should be set at a point where the derivative value increases above 3. This value has led to the segmentation results in the best way matching the expert choice.

2.2. Application of multilayer perceptron. The multilayer perceptron is the solution of a universal approximator that is

270

able to approximate any complicated input-output mapping. It is the popular neural network structure applying the sigmoidal neurons [15]. The information put to the input of network is processed locally in each unit by computing the dot product between the corresponding input vector and the weighting vector of the neuron. Training the network to produce a desired output vector when presented with an input vector involves systematically changing the weights of all neurons until the network produces the desired output (the shape of the sorted pixel intensity values) within a given tolerance. The procedure is repeated over the entire training set and the learning is reduced to the minimization of the Euclidean error measure over this set. The most effective learning approach applies the gradient information and uses the second order optimization algorithms, like Levenberg-Marquardt or conjugate gradient applications [15]. Gradient vector in multilayer network is computed using the backpropagation algorithm. As a result

of application of MLP the sorted pixel intensity sequence is approximated by the following function

$$F(x) = \sum_{i=1}^{K} w_i f(u_i) + w_0 = \sum_{i=1}^{K} w_i f(w_{i1} x + w_{i0}) + w_0 \quad (3)$$

in which $f(u_i)$ represents the sigmoidal function $f(u_i) = 1/(1 + \exp(-u_i))$, w_i $(i = 1, 2, \ldots, K)$ the weights of the output layer, w_{i1} the weights of the hidden layer, K the number of hidden sigmoidal neurons and x is the succeeding number of pixel. Similarly to the polynomial approximation derivative of this function allows to find the proper threshold level. The derivative value can be easily determined on the basis of function (3) as following

$$\frac{dF(x)}{dx} = \sum_{i=1}^{K} w_i f(u_i) (1 - f(u_i)) w_{i1}. \quad (4)$$
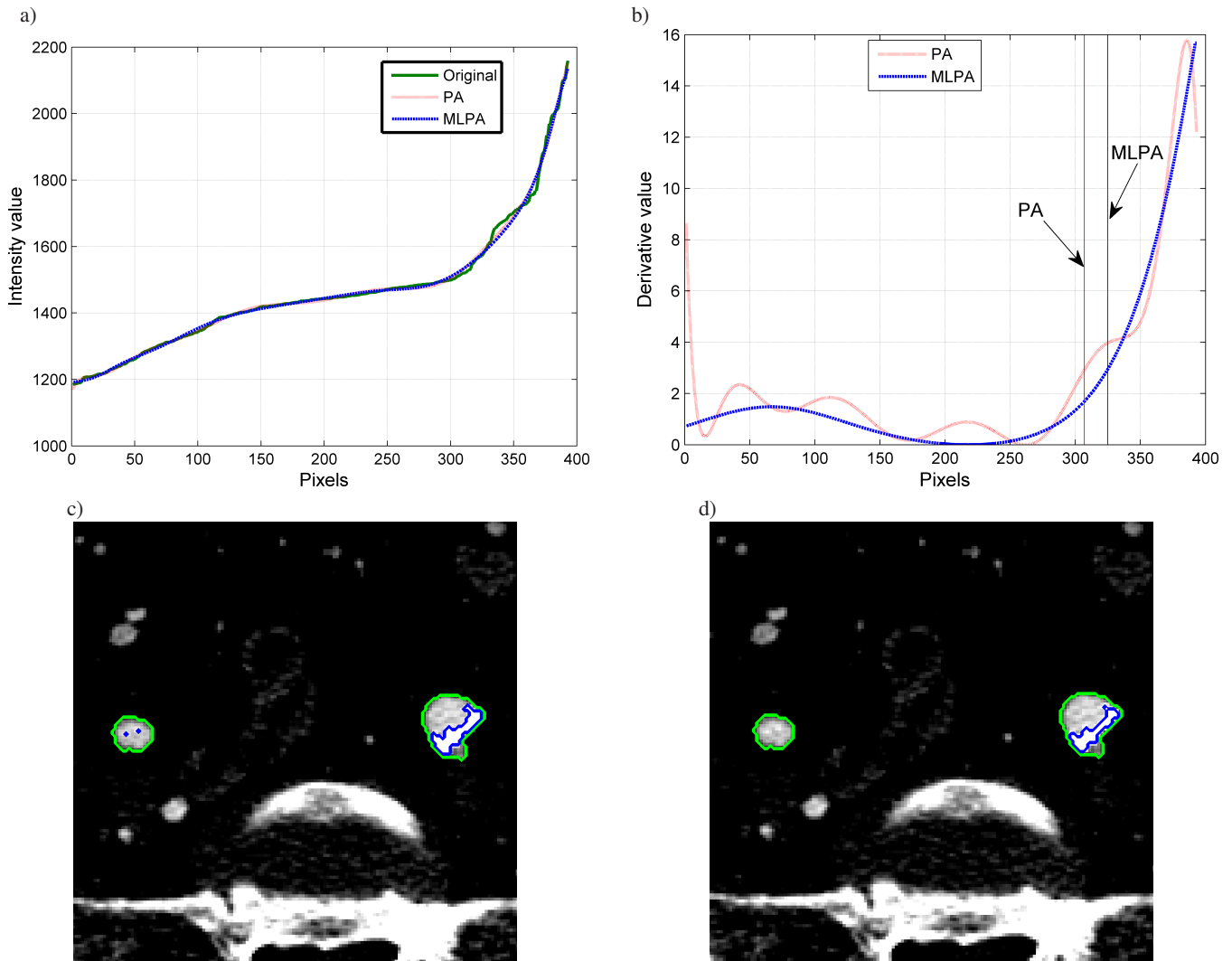

Fig. 2. The approximation approach to the segmentation: a) the polynomial function and MLP approximation of the sorted pixel intensity of the atherosclerotic artery of Fig. 1, b) their derivative functions with the threshold values pointed by the vertical lines, c) the artery area inside of the green envelope divided into lumen and plaque (white area) after application of polynomial approximation and d) after MLP approximation

We have applied this method as an alternative to the polynomial approximation. The optimal threshold corresponds to the pixel intensity in the region of the fast increase of the value of the first derivative of the approximating function. Figure 2 presents the application of both approximation approaches to the determination of the thresholding problem for the image of Fig. 1a. Figure 2a presents the shape of the polynomial approximation (PA) and MLP approximating functions (ML-PA). They differ very slightly. On the basis of their derivatives (Fig. 2b) we have got the segmented arteries (the area inside of the green envelope) divided into lumen and plaque (white area) as presented in Fig. 2c and 2d. At the assumed criterion of the first derivative (the level of 3) the optimal threshold value is set to 1513 (in polynomial approximation) and 1572 (in MLP approach). According to medical expert opinion the MLP result fits better the real division of the artery area into lumen and plaques.

2.3. The method of between-class variance. This classical algorithm is based on the statistics of pixel intensity values and was introduced by Otsu [11] for determining an optimal threshold segmenting the image into nearly uniform regions. According to the Otsu method many relevant threshold values are tried and the mean and variance of both classes as well as BCV are calculated for each of them. The bimodal gray-level histogram is normalized and regarded as a discrete probability distribution function $p(i)$ that is, $p(i) = n_i/M$, where n_i is the frequency of the gray level i and M is the total number of pixels in the image. If the histogram is divided into two classes by the gray-level intensity t (potential threshold), then the probabilities of the respective classes can be expressed as

$$p_1(t) = \sum_{i=0}^{t} p(i), \tag{5}$$

$$p_2(t) = \sum_{i=t+1}^{N-1} p(i). \tag{6}$$

Denoting by $m_1(t)$, $m_2(t)$ the means of these two classes at the actual threshold value t, where $m_j = \sum_{i=0}^{t} ip(i)/p_j(t)$ ($j = 1, 2$) the value of BCV is defined in the form [11]

$$BCV(t) = p_1(t)p_2(t)\left(m_2(t) - m_1(t)\right)^2. \tag{7}$$

Application of BCV criterion to the determination of the optimal threshold of the image of Fig. 1a has generated the value equal 1670, significantly different from both approximation approaches.

2.4. K-means clustering. The unsupervised classification, called clustering, can be also used to provide the natural grouping of the multidimensional data set. This approach requires to determine the initial number of classes K and initial positions of their centroids. The adaptation of cluster centers is done by minimizing the sum of the within-cluster variances [15]

$$Q = \sum_{j=1}^{K} \sum_{i=1}^{n} \left\| \mathbf{v}_i^j - \mathbf{c}_j \right\|^2, \tag{8}$$

where $\mathbf{v}_i^j$ is the i-th image sample of j-th class and $\mathbf{c}_j$ the center defined as the mean of $\mathbf{v}_i^j \in K_j$. The K-means [15] assumes that each vector $\mathbf{v}_i$ belongs to only one cluster $\mathbf{c}_j$. There exists also the generalization of K-means in the form of so called fuzzy C-means [15] in which the vector $\mathbf{v}_i$ belongs simultaneously to all classes with some membership values changing from zero to one.

The idea of application of clustering to the segmentation is to pick a threshold such that each pixel on each side of the threshold is closer in intensity to the mean of all pixels on that side than the mean of all pixels on the other side of the threshold. Since the ranges of pixel intensities of both regions usually overlap, the algorithm tries to minimize the area under the histogram for one region that lies on the other region's side of the threshold. Application of K-means clustering to the image of Fig. 1a has resulted into the value of threshold equal 1632.

2.5. Gaussian mixture modeling. Thresholding based on the mixture modeling assumes that the pixel values forming each group are Gaussian distributed. The modes are the bumps in the image histogram and correspond to the certain regions of the image, where the number of pixels attaining those values are relatively high. Assuming the existence of K groups of pixels, each characterized by its mean m_i ($i = 1, 2, \ldots, K$) and appropriate standard deviation σ_i independent on the threshold, the model of pixel value distribution may be described by

$$f(x) = \sum_{i=1}^{K} A_i e^{-(x-m_i)^2/2\sigma_i^2}. \tag{9}$$

Identifying the probability density function (pdf) parameters of the pixel intensity values of the whole image we can use this knowledge to find the probability of any pixel value belonging to different groups (modes) of the image. Mixture modeling is a technique for estimating the pdf of pixel values belonging to different classes. In this method the pdf of pixel distribution is estimated as a frequency of occurrence of this grey level in the histogram of the image. If we have K modes (classes) in the pdf of pixel values we may say, that x may come from any of those K densities with different probability.

The initialization of the classes is usually started by applying K-means clustering. Once a mixture model is fitted to the image pdf, we can assign pixels to different classes on the basis of the final estimated posterior probabilities, i.e. assigning the pixel x_j to the class that produces the highest value of probability. The details of this approach can be found in [14]. This method of segmentation will be called further GMM. Applying this method of thresholding to the image of Fig. 1a we have found the optimal threshold value equal 1543, very close to both approximation approaches.

2.6. Comparative analysis of methods for identification of atherosclerotic plaque areas. In the first step of comparison we present the exemplary results of division of the artery area into lumen and atherosclerotic plaque regions by using different methods of thresholding. Figure 3 depicts the graphical presentation of the results of separation of both (left and right) arteries in one slice image of the patient (Fig. 3a) into two regions: the lumen and calcified plaques by applying the polynomial approximation (Fig. 3b), MLP approach (Fig. 3c), BCV (Fig. 3d), K-means clustering (Fig. 3e) and GMM (Fig. 3f). The brown lines represent the circumference of the localized artery and the area inside the dark blue envelope – the plaque regions. As it is seen the most compatible results of segmentation (the size, shape and location of plaques) correspond to the application of GMM and MLP.

The same task of segmentation was performed by the medical expert, who has drawn manually the regions of lumen and plaques in the analyzed image. According to him the most accurate division into lumen and plaque areas has been obtained by the MLP approximation and GMM methods.

In a general case the automatic identification of atherosclerotic changes creates two tasks: the estimation of the number of classes and recognition of regions of artery belonging to each class. Both tasks are strictly connected with each other.

In general, three types of the atherosclerotic changes should be taken into account.

1. All pixels represent artery lumen with contrasted blood: the simplest case – only one recognized class (the lumen).
2. Some pixels represent artery lumen and some calcified atherosclerotic plaque areas – two classes for recognition (the first class – lumen and the second – calcified plaques).
3. Some pixels represent artery lumen, some calcified atherosclerotic plaques and some – the non-calcified plaques (most often lying between the first two) – three classes for recognition (class 1 – lumen, class 2 – calcified plaques and class 3 – non-calcified plaques).

However, the great changes of the intensity values within each class of the MSCT images constitute a problem, not only between slices belonging to different patients, but also within the sequence of slices for the same patient. This is the result of different distribution of contrast in the arteries. The observed differences of the threshold values at recognition between artery lumen and calcified plaque were quite large (for example 1416 in the first slice, 1540 in the second and 1630 in other slices, all generated by the same method for the same patient).
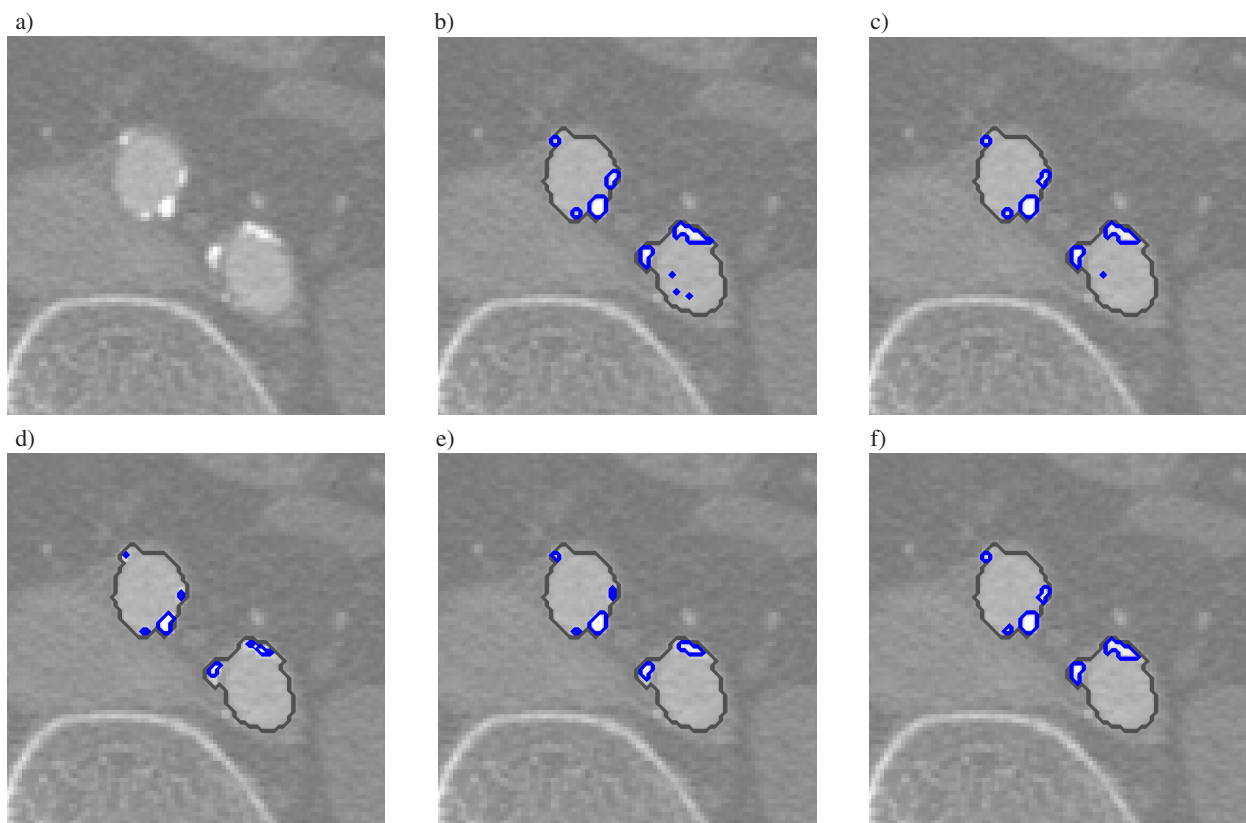

Fig. 3. The graphical results of segmentation of the image of the left and right arteries into lumen and calcified plaque regions: a) original image, and the results of b) polynomial approximation, c) MLP, d) BCV, e) K-means clustering, f) GMM methods
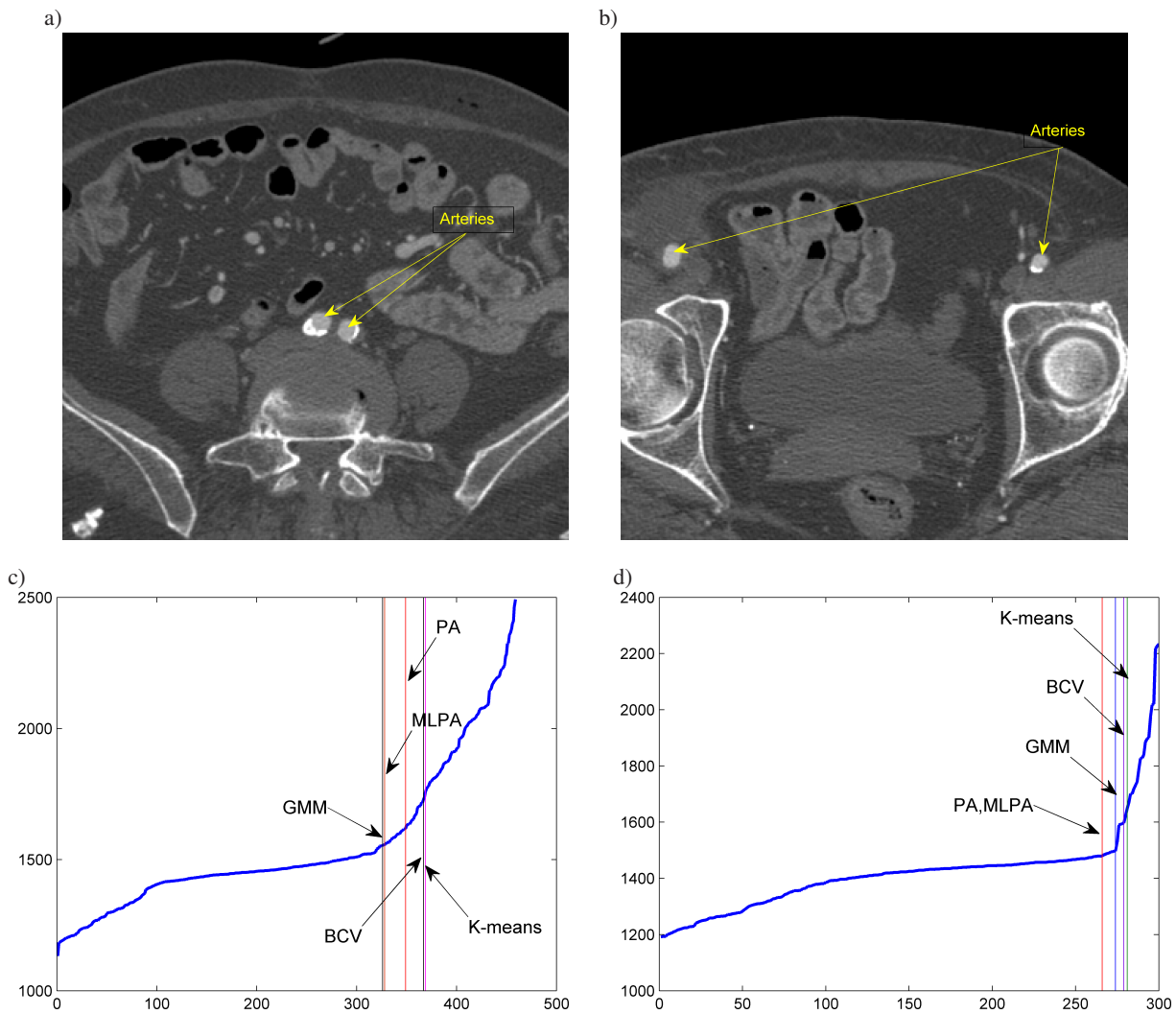
Fig. 4. The comparative results of segmentation of two cases: a) the view of the iliac artery slice and b) external iliac artery passing into femoral artery, c) the threshold values for the iliac and d) for external iliac artery, estimated by different methods

Figure 4 shows the results of thresholding two images of iliac (Fig. 4a) and external iliac passing into femoral (Fig. 4b) arteries at application of different methods: polynomial approximation (PA), multilayer perceptron approximation (ML-PA), Gaussian mixture modeling (GMM), BCV and K-means clustering represented in Fig. 4c and 4d. The horizontal axis represents the pixels arranged in increasing order, and the vertical axis presents their intensity values. The positions of optimal thresholds pointed by different methods are represented by the vertical lines in Figs. 4c and 4d, respectively.

As we can see the application of different methods results in different values of optimal threshold. Close analysis of many slice images have revealed that GMM and MLP approximation produce the most stable and accurate threshold values and are closest to the human expert choice. Therefore in further analysis only these two approaches are used.

Let us assume now the most general case considering the division of artery plane into 3 regions. In the case of application of PA it is reflected by 2 sections of the highest slope of sorted pixel intensity separated by the middle one of the

significantly lower slope. In the case of GMM we identify three bumps in the histogram of pixel intensities.

In general case we should assume 3 regions (classes) existing in the artery: the lumen, calcified plaques and non-calcified plaques. The automatic class recognition has been obtained in our solution by adding the step of evaluating the variances of the intensity of pixels within each region. On the basis of the performed experiments we have found that if the variance of pixels belonging to the region of the largest mean is smaller than 3000, then the calcified atherosclerotic plaques are not present in this region and all pixels represent the artery lumen (one class region). In the other case, pixels of this region represent calcified atherosclerotic plaques (the non-calcified plaques should be placed only in region of lowest means). If the second case happens (the considered pixels represent the calcified plaques) we have to decide if the middle region represents the lumen or also the calcified plaques. To solve this dilemma we have applied again the observations regarding the variance of pixel intensities.
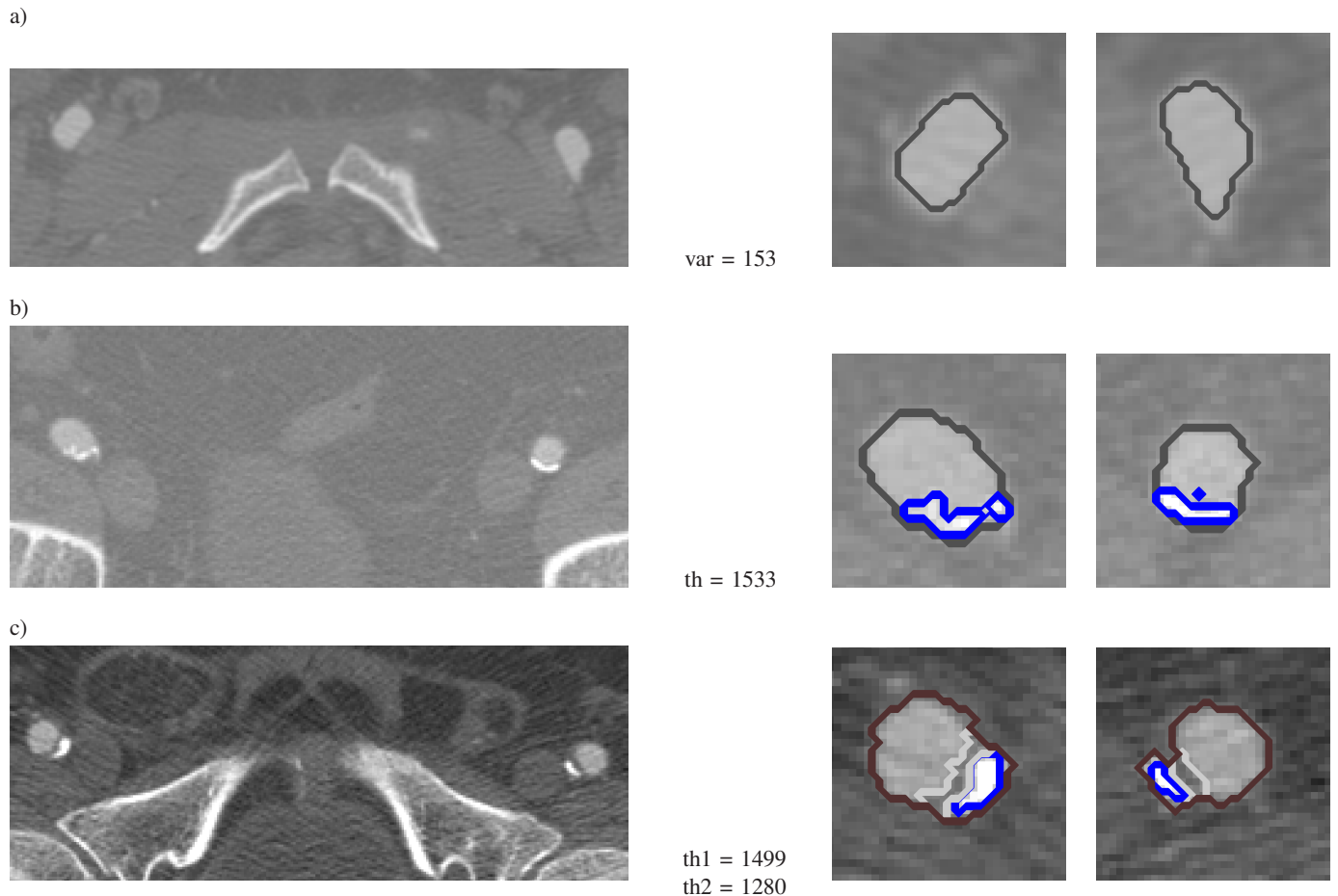
a)

b)

c)

Fig. 5. The results of recognition of the lumen and plaques areas in the arteries: a) only lumen recognized, b) lumen and calcified plaques (the blue color), c) lumen, calcified plaques (blue color) and non-calcified plaques (yellow color). The middle column shows the variance (in the first case) and threshold values applied in the division of the artery areas

When the variance of pixel intensity in the middle region is greater than 10000 it represents the calcified plaque; in the other case – the lumen area. When the middle region represents plaque area, the class of the lowest mean represents lumen. However, when the middle class is interpreted as the lumen, the region of the curve with lowest mean value should be statistically evaluated and then recognized either as a lumen (if variance is small) or non-calcified atherosclerotic plaque area in other case.

Figure 5 presents the results of segmentation of MSCT images at different advancement of atherosclerosis. The first row (a) depicts a fragment of a slice image containing the arteries without plaques. The variance of the sorted pixel intensity was equal 153 being the evidence of only lumen existence. The second row depicts the situation of splitting the artery area into lumen and calcified plaques. The optimal threshold value in this case was equal 1533. The last row (c) represents the case with three regions: lumen, calcified plaque region (white) encircled by the blue envelope and non-calcified plaque area encircled by white line. In the last case there were 2 threshold values equal th1 = 1499 and th2 = 1280, used to separate lumen, calcified and non-calcified plaques.

3. Results and discussion

3.1. The analyzed data base. The performance of an automatic system of the atherosclerotic changes identification and quantization in the vascular arteries was checked on the data base of MSCT slice image sequences obtained for 128 patients at different stages of atherosclerotic changes in the iliac and femoral arteries. The cases were collected by the vascular surgery experts from the Department of Vascular Surgery of Military Institute of Medicine, Warsaw, within the patients who were the candidates for the endovascular or surgical intervention.

The age of the patients ranged from 40 to 86 years (average 65 years) and the MSCT images were collected within the years 2006–2010. Effectively 434 segments of the arteries were distinguished and analyzed. Only the arteries with continuous MSCT imaging of their lumen were taken into account. The cases of not continuous artery lumen or with aneurysm were not evaluated in this study. All images were collected by using the 64-slice General Electric (Fairfield, CT, USA) MSCT. Computed tomography of iliac and femoral arteries was performed with a standardized

optimized contrast-enhanced protocol (120 kVp, 180 mAs, collimation 64×0.625 mm, pitch 0.5). All patients received 150 ml contrast material (Iomeron 400 mg/ml Bracco, UK) with SmartPrep. Image reconstructions were made with a 250 mm field of view, a matrix size of 512×512, a slice thickness of 0.625 mm, an increment of 0.625 mm, and at application of standard reconstruction filter. The MSCT images were stored in DICOM format ver. 3.

3.2. Comparison of automatic results of segmentation with the human experts. In further analysis we concentrate on two methods: the MLP approximation of the sorted pixel intensities and Gaussian mixture modeling found by us as the most successful in analyzing the atherosclerotic cases.

In the first experiments we have selected 300 slices coming from one patient, for whom we made the manual assessment (done by experts) regarding the number of the classes and proper ranges of the threshold values, to get the acceptable recognition between artery lumen and plaques. The comparison of results of an automatic segmentation with MLP approximation and GMM methods will be presented first in a graphical form. To increase the stability and accuracy of results of the thresholding procedure and to involve the actual experience into the processing of the image sequence we have additionally applied the on-line adaptation of the threshold value for the next slice by taking the average of six last ap-

plied threshold values. The comparative results, concerning the rate of decrease of the artery lumen for the succeeding 300 slice images of one patient are presented in Fig. 6.

It is seen that all applied methods produce the results, which are well compatible with each other. The general trend of the change of the lumen decrease was the same for all of them, although there are some small local discrepancies.

Table 1 presents the mean values of the rate of decrease of the lumen for all analyzed slice sequences of Fig. 6. We relate the results of our two methods of an automatic threshold determination and the results of the manual adjustment of the threshold value made by two experts. The difference between them is treated as an estimation error.

The presented results show that practically in all cases the application of MLP and GMM with the adaptive adjustment of the threshold has led to the estimation error of very small values. Fully acceptable is also the level of the maximum absolute error of estimation, caused by the single missegmentation, that may happen sometimes. The observed decrease of the mean error for all slices under investigation, obtained thanks to application of the adaptation technique, is on the level of 30% (in comparison to the fixed value of threshold). Comparing GMM and MLPA we may note some superiority of MLPA (0.15% and 0.42% of mean errors compared to 1.95% and 1.38% of GMM).
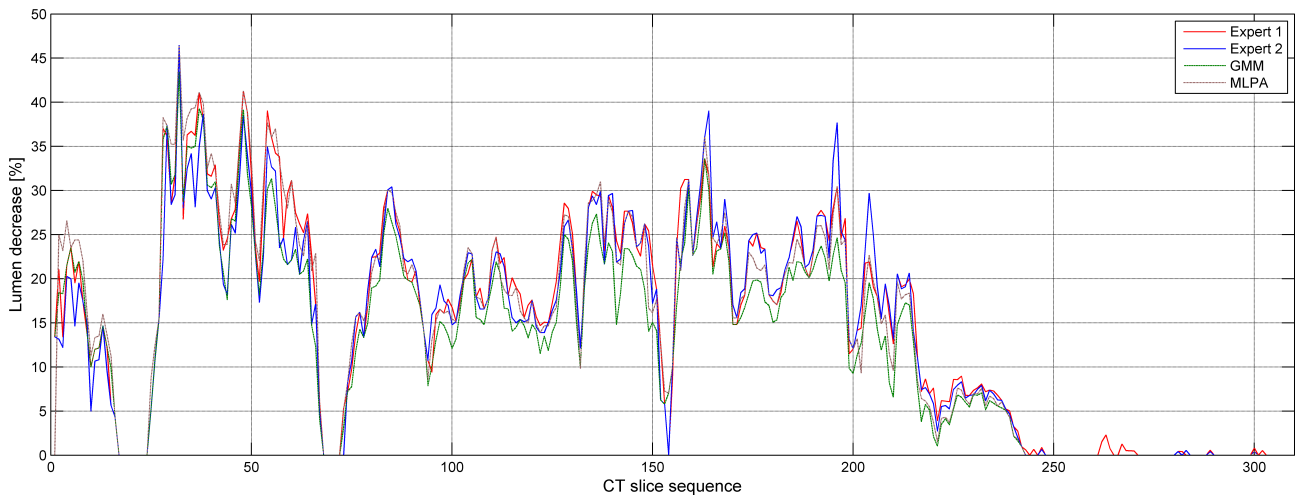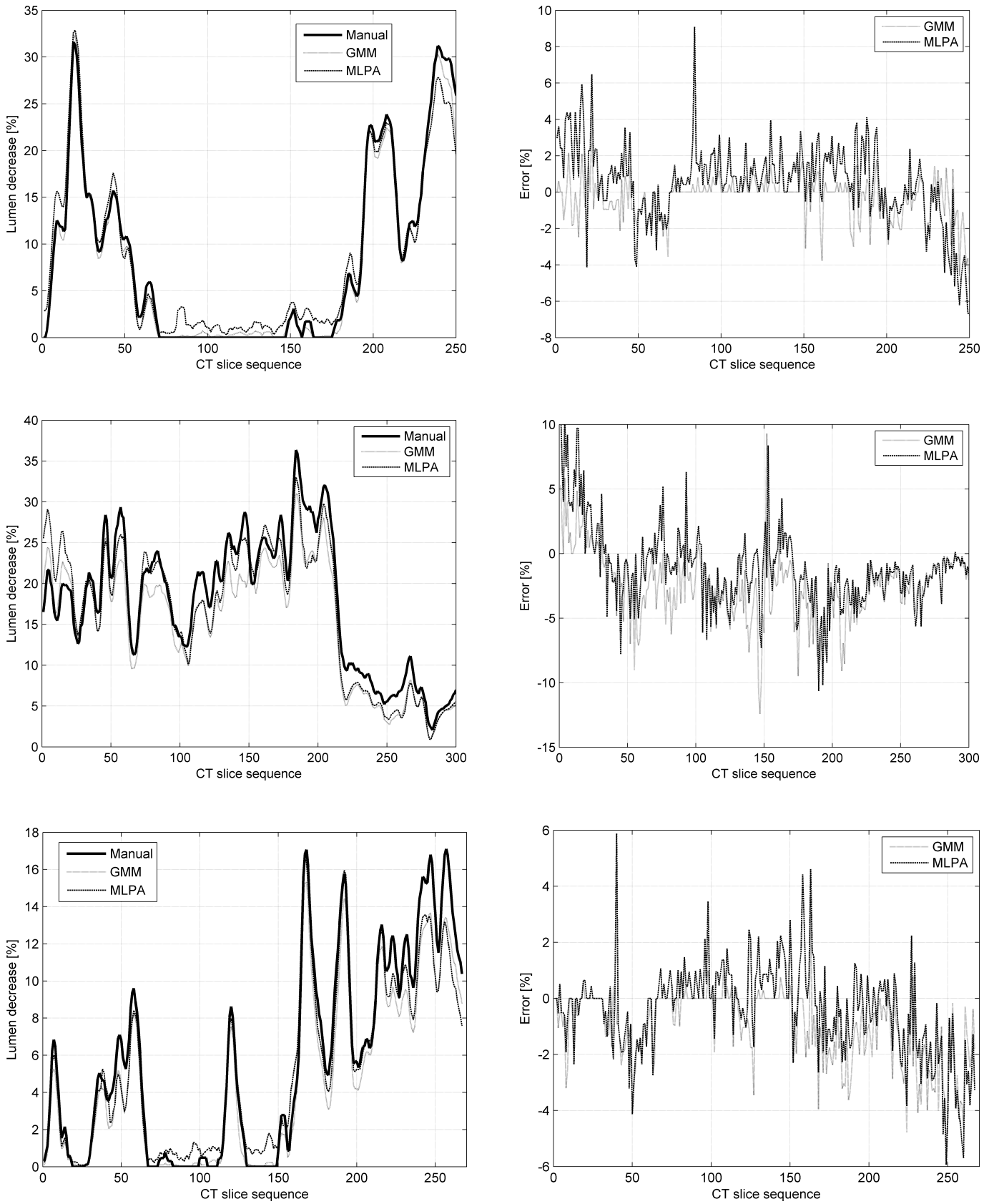

Fig. 6. The comparison of the artery lumen decrease rate for the MSCT slice sequence at application of GMM and MLPA methods and 2 medical experts

Table 1
Numerical comparison of the artery lumen decrease evaluation

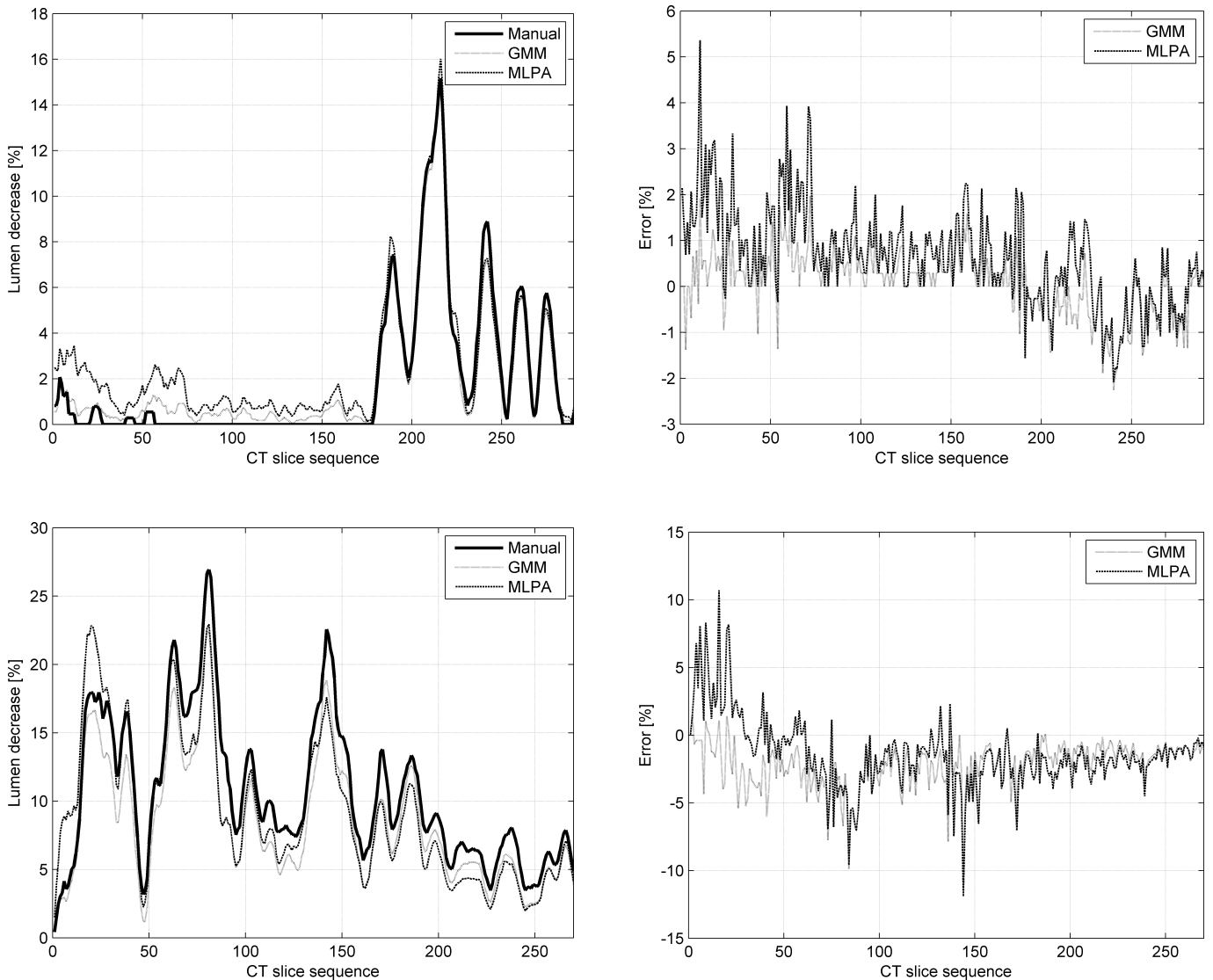|	Expert 1 as a reference				Expert 2 as a reference		
	Mean lumen decrease [%]	Mean error [%]	STD of error	Max absolute error [%]	Mean error [%]	STD of error	Max absolute error [%]
Expert 1	15.27	–	–	–	0.57	2.08	14.81
Expert 2	14.70	0.57	2.08	14.81	–	–	–
GMM	13.32	1.95	2.44	11.40	1.38	2.77	13.58
MLPA	15.12	0.15	2.15	13.41	0.42	3.02	13.41

[Fig. 7]

Fig. 7. The comparison of the artery lumen decrease evaluation for sample series of the MSCT images at application of the moving average over 5 slices. The presented results are related to MLPA, GMM and human expert. Left column presents the lumen decrease (in %) and the right one the corresponding difference between our automatic methods and manual human expert estimations [colour on-line]

In medical practice the important is the decrease of the lumen averaged over few slices. Taking into account that the thickness of single MSCT slice is 0.625 mm, the total thickness over 5 slices corresponding to approximately 4 mm length was taken as a standard. We have applied such moving average of the results and compared it with the manual results of the expert. Figure 7 presents the graphical comparison of lumen decrease in the sequence of MSCT slices for 5 exemplary cases corresponding to five different patients. The results represent the moving average of lumen decrease at application of the window equal 5 (the left column) and the error of estimation of this decrease with respect to the manual assessment of the expert, treated as the reference (the right column of the figure). The curves compare the results of application of MLPA (dashed line), GMM (dot line) and the manual assessment made by the human expert (solid line).

The average error of estimation of the lumen decrease (measured in percentage) for all slices of these 5 images (over 1000 analyzed images) was equal to 1.64% at the application of MLP approximation and 1.71% for GMM approach.

3.3. The numerical characterization of the pathology of artery. The results of the computer segmentation of the artery allow to characterize the atherosclerotic changes in the numerical way by using additional mathematical tools based on the statistics. The most important factor is the level of decrease of the artery lumen, defined as a ratio between the artery lumen (the area without recognized atherosclerotic plaques) and the total area of lumen and plaques taken together. The other measure is defined on the basis of the area of ellipse described on the recognized artery. This area is treated as the approximation of the original lumen area. The ellipse is characterized by the length of the major and minor axes.

On the basis of the above discussion the following statistical descriptors for numerical evaluation of the atherosclerotic changes in four anatomical parts (iliac and femoral branches and iliac and femoral common arteries) can be defined:

F1 – Mean artery lumen decrease [%],

F2 – Maximum artery lumen decrease [%],

F3 – Mean artery lumen area [mm^2],

F4 – Minimum artery lumen area [mm^2],

F5 – Mean lumen decrease in femoral artery [%],

F6 – Mean lumen decrease in iliac artery[%],

F7 – Mean lumen decrease related to the ellipse area in the femoral artery [%],

F8 – Mean lumen decrease related to the ellipse area in the iliac artery [%],

F9 – The percentage of the plaque participation in the MSCT image sequence.

They represent the most interesting measures from the medical point of view useful for finding points in arteries, crucial from the surgical point of view. All these parameters can be determined only by the computerized system, since it is practically impossible to do it manually by an expert. In the final investigations of the atherosclerotic plaques we have used the whole data base of 121 patients selected by medical experts.

In the first case we limit the presentation of detailed numerical results concerning these measures to the MSCT sequences of only 10 randomly selected patients, as presented in Table 2, in which the notation R refers to the right and L to the left artery.

Table 2
The collected quantitative evaluation of the atherosclerosis for the set of 10 patients (2689 images)

No of patient	Artery	F1	F2	F3	F4	F5	F6	F7	F8	F9
1	R	12.1	32.4	130.5	27.1	9.3	22.6	11.1	27.5	79.1
	L	10.3	31.4	129.7	10.6	7.9	22.5	10.6	38.0	72.0
2	R	0.2	10.2	70.4	35.1	0.0	0.4	1.7	8.7	3.1
	L	0.0	4.5	66.2	24.7	0.1	0.0	2.7	1.4	1.7
3	R	3.0	25.7	48.1	25.8	0.1	17.3	1.8	24.0	20.7
	L	0.7	18.1	49.4	20.3	0.0	4.5	1.5	9.5	8.1
4	R	8.4	33.8	172.8	69.6	6.8	11.1	8.8	14.8	67.1
	L	9.3	45.1	143.1	73.2	8.5	20.7	10.7	27.9	41.8
5	R	1.4	23.8	49.0	12.1	1.4	1.3	4.3	5.2	19.1
	L	1.5	25.3	56.7	15.2	0.5	3.8	4.0	8.5	19.8
6	R	9.0	35.4	163.4	62.1	8.0	10.3	10.6	14.7	70.9
	L	11.0	47.2	136.7	70.4	9.7	21.1	11.7	26.7	47.5
7	R	10.5	58.9	79.0	23.1	11.6	8.4	21.0	12.2	78.2
	L	5.2	28.4	79.6	31.9	4.2	9.3	7.8	13.1	54.4
8	R	16.9	76.0	97.0	26.1	11.0	36.2	13.8	45.2	68.9
	L	12.5	69.0	110.4	16.7	8.1	11.0	11.0	35.8	81.9
9	R	4.6	24.7	106.6	35.4	1.3	9.7	3.4	11.5	51.5
	L	3.4	29.7	75.7	19.1	1.2	8.8	3.4	11.4	40.3
10	R	13.3	31.6	123.1	44.0	14.5	8.3	18.9	11.5	94.7
	L	9.3	25.8	138.7	34.6	10.0	6.7	13.0	16.4	93.0
Mean		7.1	33.9	101.3	33.9	5.7	11.7	8.6	18.2	50.7

It is a general opinion, that the ellipse approximation of the artery plane is more restrictive than the real area of artery. It has been confirmed by the numerical results concerning the values of F7 and F8 measures. As a result of introducing the ellipse approximation, the average artery lumen decrease measure has changed from 5.7% (F5) to 8.6% (F7) for the iliac and from 11.7% (F6) to 18.2% (F8) for the femoral artery.

The next results concerning the statistics of the left and right arteries parameters (from F1 to F9) have been established for all 121 patients considered in the experiments. They are presented in Table 3 in the form of mean values and standard deviations as well as the ranges of their changes within this group of patients. The results show that these measures are varied in a very wide range for different patients, according to the advancement of the atherosclerotic changes. However, we have not observed the significant differences corresponding to the left and right arteries. The specific results comparing the clinical evaluation of the atherosclerotic changes obtained by using our system will be presented in the other, more clinically oriented paper.

Table 3
The summary of the quantitative automatic evaluation of the arteries for all 121 patients (∼270 images per patient)

	Right artery		Left artery	
	mean±std	range	mean±std	range
F1	6.44±6.69	0–27.6	6.28±7.12	0–34.9
F2	33.34±22.52	2.2–98.4	33.32±21.15	0–94.8
F3	87.14±41.72	22.5–201.4	82.33±42.49	23.4–207.0
F4	25.76±13.11	1.0–69.6	26.18±15.35	2.6–73.2
F5	4.90±6.46	0–35.1	4.66±6.24	0–37.9
F6	11.10±11.20	0–47.4	10.74±11.31	0–60.4
F7	8.67±8.10	1.0–48.6	8.10±7.16	0.3–39.1
F8	16.18±13.33	0.4–70.6	16.06±13.86	0.5–81.0
F9	42.70±26.34	1.3–99.6	41.56±26.61	0–99.3

4. Conclusions

The paper has presented and compared different approaches to the image segmentation by using thresholding. We have compared such methods as BCV, GMM, clustering approach and application of polynomial and MLP approximations of the sorted pixel intensities. On the basis of many numerical experiments concerning segmentation of the iliac and femoral artery areas in the images of the MSCT slice sequences we have found that MLP approximation and GMM provide the most accurate and repeatable results of recognition between lumen and atherosclerotic plaque regions. The results of such recognition are applied in the numerical parameterization of the atherosclerotic changes and the paper presents some chosen results of such analysis.

The approach presented in the paper may be applied to in vivo MSCT image sequence of the femoral and iliac artery vessels to identify and estimate artery atherosclerosis plaque burden and its feature parameterization. The segmented images can be used in major vessels to evaluate the risk of

atherosclerosis. The results of our investigations may be also helpful for medical experts in solving many problems of vascular MSCT imaging such as: isolation of plaques from the lumen region or multiple lesions in the artery, percentage occlusion or narrowing of lumen in vascular segment as well as localization of the occlusion in the artery.

REFERENCES

[1] E.G. Bovenkamp, J. Dijkstra, J.G. Bosch, and J.H. Reiber, "Multi-agent segmentation of IVUS images", *Pattern Recogn.* 37 (4), 647–663 (2004).

[2] N. Passat, C. Ronse, and J. Baruthio, "Region-growing segmentation of brain vessels: an atlas-based automatic approach", *J. Magn. Reson. Imaging.* 21 (6), 715–725 (2005).

[3] N. Passat, C. Ronse, and J. Baruthio, "Watershed and multi-modal data for vessel segmentation: application to the superior sagittal sinus", *Image Vision Comput.* 25 (4), 512–521 (2007).

[4] P. Soille, *Morphological Image Analysis, Principles and Applications*, Springer, Berlin, 2003.

[5] Y. Shang, R. Deklerck, E. Nyssen, A. Markova, J. de Mey, X. Yang, and K. Sun, "Vascular active contour for vessel tree segmentation", *IEEE Trans. Biomed. Eng.* 58 (4), 1023–1032 (2011).

[6] T. Markiewicz, P. Wisniewski, and S. Osowski, "Comparative analysis of the methods for accurate recognition of cells in the nuclei staining of the Ki-67 in neuroblastoma and ER/PR status staining in breast cancer", *Anal. Quant. Cytol. Histol.* 31 (1), 49–62 (2009).

[7] B. Raman, R. Raman, G.D. Rubin, and S. Napel, "Automated tracing of the adventitial contour of aortoiliac and peripheral arterial walls in CT angiography (CTA) to allow calculation of non-calcified burden", *J. Digit Imaging* 24 (6), 1078–1086 (2011).

[8] T. Schepis, M. Marwan, T. Pflederer, M. Seltmann, D. Ropers, W.G. Daniel, and S. Achenbach, "Quantification of non-calcified coronary atherosclerotic plaques with dual-source computed tomography: comparison with intravascular ultrasound", *Heart* 96 (8), 610–615 (2010).

[9] G. Korosoglou, D. Mueller, S. Lehrke, H. Steen, W. Hosch, T. Heye, H.U. Kauczor, E. Giannitis, and H.A. Katus, "Quantitative assessment of stenosis severity and atherosclerotic plaque composition using 256-slice computed tomography", *Eur. Radiol.* 20, 1841–1850 (2010).

[10] J. Kittler, J. Illingworth, "Minimum error thresholding", *Pattern Recogn.* 19 (1), 41–47 (1986).

[11] N. Otsu, "A threshold selection method from grey-level histograms", *IEEE Trans. Sys. Man. Cyb.* 9 (1), 62–66 (1979).

[12] S.S. Reddi, F.S. Rudin, and H.R. Keshavan, "An optimal multiple threshold scheme for image segmentation", *IEEE Trans. Sys. Man. Cyb.* 14 (4), 661–665 (1984).

[13] T. Kurita, N. Otsu, and N. Adbelmalek, "Maximum likelihood thresholding based on population mixture mode", *Pattern Recogn.* 25 (10), 1231–1240 (1992).

[14] O. Demirkaya, M.H. Asyali, and P.H. Sahoo, *Image Processing with MATLAB: Applications in Medicine and Biology*, CRC Press, Boca Raton, 2009.

[15] S. Osowski, *Methods and Tools of Data Mining*, BTC, Warszawa, 2013, (in Polish).